



WALL-TO-FLOOR INTERACTION IN RC BUILDINGS: MODELLING CASE STUDY

E. R. Encina⁽¹⁾, R. S. Henry⁽²⁾

⁽¹⁾ PhD Candidate, University of Auckland, eenc456@aucklanduni.ac.nz

⁽²⁾ Senior Lecturer, University of Auckland, rs.henry@auckland.ac.nz

Abstract

Current methods of seismic analysis and design of reinforced concrete (RC) buildings typically consider the walls in isolation from the rest of the building, or rely on rigid diaphragm constraints. However, recent research on wall-to-floor interaction has shown that the coupling between the lateral load resisting system and the gravity system may alter the seismic response of the building and increase design actions on RC walls. Additionally, wall-to-floor interaction can also restrict the elongation of the plastic hinge of the walls, resulting in an increase in wall axial load. To investigate the effects of wall-to-floor interaction, a case-study building that represented a common building typology was modelled. The lateral load resisting system in one direction of the case-study building was composed of a RC wall with columns in close proximity to the ends of the wall. Non-linear fibre-based models were developed representing the lateral load resisting system and a series of pushover analyses were conducted to investigate the effects of interactions between the wall, floor, and columns. The results showed that the interactions increased the system lateral load capacity by approximately 15% when compared to a model without interaction or coupling between members. In addition, the wall shear and axial demands increased by 13% and 49% respectively. A series of parametric analyses highlighted a high dependency on the geometry of the members and layout. Increases of up to 45% of the system lateral load strength and between -200% and +84% of the column axial load were observed.

Keywords: RC wall; wall-to-floor interaction; reinforced concrete; nonlinear modelling; unintentional coupling, wall elongation

1. Introduction

A significant number of mid- and high-rise reinforced concrete (RC) buildings in seismic regions use structural walls as the primary lateral load resisting system. By following capacity design procedures, ductile RC walls can be designed to ensure that a flexural plastic hinge forms to allow the wall to withstand large lateral displacements [1]. Typically the analysis that is conducted to determine the design lateral load demands considers the walls working in isolation from the gravity load resisting system. However, some researchers have shown that the floor systems may couple the wall response with the surrounding gravity system [2-4]. As a result of this unintentional coupling (wall-to-floor interaction), the demands in both the lateral load resisting system and the gravity system may be altered.

Floor systems may provide constraints between vertical structural elements in both an in-plane and an out-of-plane orientation. Investigations on the in-plane behaviour of floors interacting with RC walls have focused on the in-plane flexibility of the floor diaphragm system [5-7] and the design of diaphragms for inertial and transfer forces [8]. Research results have highlighted the effects of diaphragm flexibility on the dynamic response of the structure and have proposed suitable methods to design the floor system to withstand the seismic-induced forces. Research on interaction caused by the out-of-plane behaviour of floors has analysed wall-to-wall and wall-to-column configurations. Investigations on wall-to-wall coupling have focused on floor slab design and behaviour [9-11], and on the lateral response of the coupled system [12-14]. Design charts to determine equivalent effective slab widths have been proposed, in addition to reinforcement detailing to delay or preclude floor damage around wall ends. Research related to the interaction between walls and the gravity system (e.g. wall-to-column) have shown both experimentally [2, 4] and analytically [3, 15, 16] that the columns or gravity load resisting frames act as outriggers that contribute to the lateral strength and stiffness of the building by the coupling mechanisms shown in Fig. 1. A drawback of the outrigger effect is that the loads generated could be substantially different to what may have been assumed in the design, with increased axial and shear forces in the wall and modified axial loads in the columns. Additionally, the floors can restrain the wall rotation and axial elongation of the plastic hinge further increasing the demands on the wall. These responses not only may affect the global behaviour (building strength and stiffness) but also the local response of the wall.

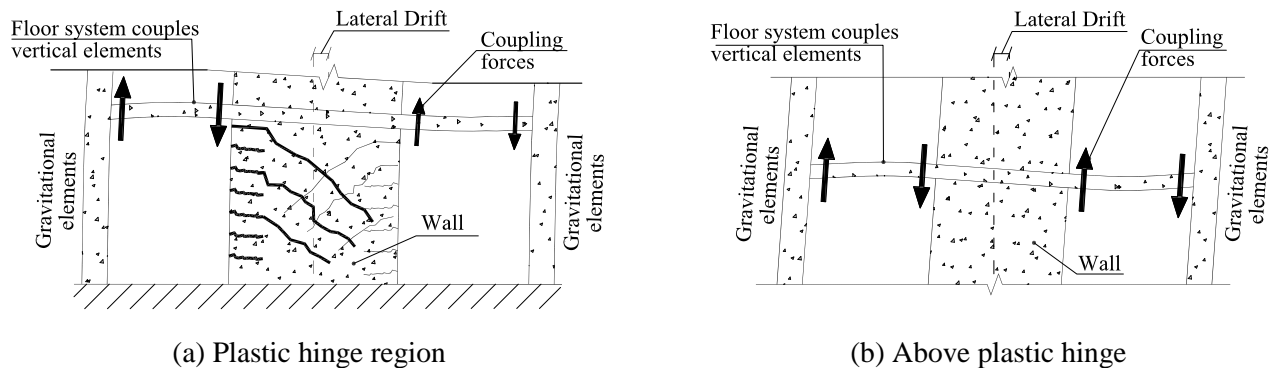


Fig. 1 – Coupling mechanisms

In order to provide guidance on seismic design actions that include consideration for structural interactions, robust numerical models need to be developed that can capture the non-linear behaviour of full building structural systems. A 2D numerical model was developed for a case study building that represented a common building typology consisting of an RC wall coupled to gravity load resisting column. Inclusion of the floor diaphragm allowed for the effects of wall-to-floor interaction to be quantified from a pushover analysis.

2. Case study building

The case study building used for this investigation was a 8-storey RC wall building with a rectangular floor plan. The building footprint was 44 m wide by 50 m long. The inter-story height was 3 m in the basement, 4.8 m in the ground level and 4.25 m in the upper levels. The lateral load resisting system consisted of four moment resisting

concrete frames in the East-West (E-W) direction and two RC walls in the North-South (N-S) direction. The floor system was constructed with pre-cast (PC) floor units with an insitu concrete topping. A schematic representation of the building floor plan and an elevation of the RC wall are shown in Fig. 2.

The RC walls were 300 mm thick, 11800 mm long and extend the full height of the building (44 m). Details of the wall section reinforcement are provided in Fig. 3(a). The longitudinal reinforcement of the wall ends at the ground level consisted of 20 layers of 3×25 mm diameter bars spaced at 100 mm centres confined by 12 mm diameter stirrups spaced at 150 mm centres. Longitudinal reinforcement in the central web region of the wall at the ground level consisted of 25 mm diameter bars spaced at 300 mm centres on each face. Horizontal wall reinforcement at the ground level consisted of 20 mm diameter bars spaced at 200 mm centres. From level 1 to 3 the reinforcement layout was maintained, but the number of bars in each layer of longitudinal reinforcement at the wall ends reduced to 2 bars. Levels 4 to 6 retained the same reinforcement layout as for levels 1 to 3, but the longitudinal bar diameter was reduced to 20 mm and the spacing of the horizontal reinforcement was increased to 300 mm.

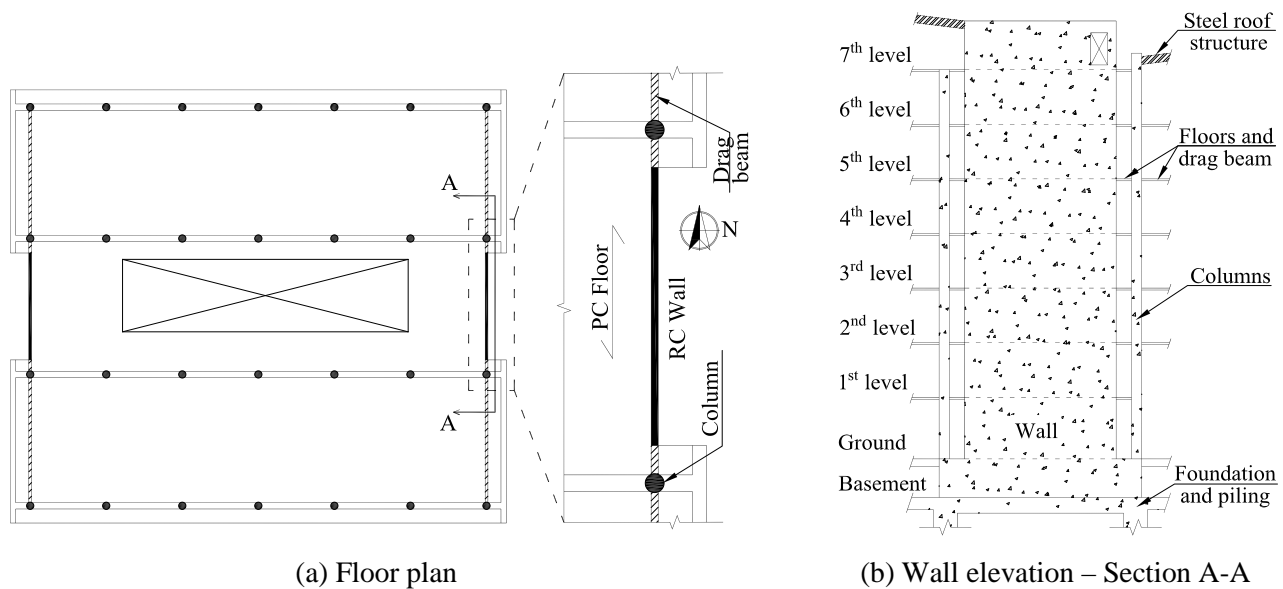


Fig. 2 – Drawings of the case-study building

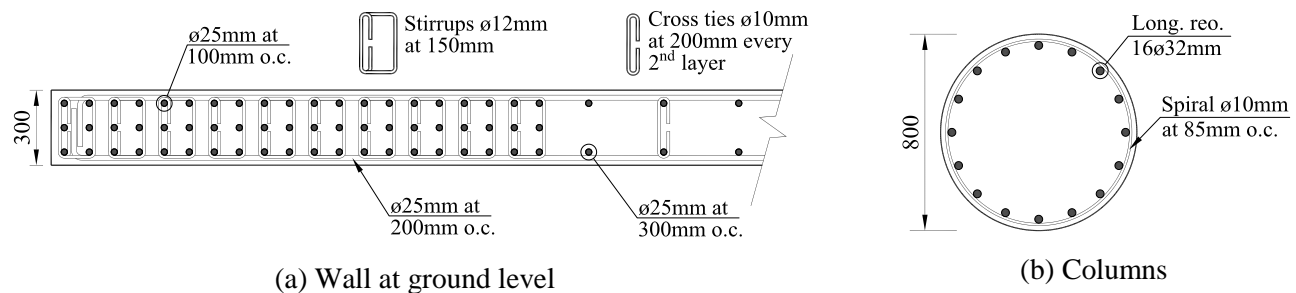


Fig. 3 – Reinforcement layout for the wall and columns

The columns were 800 mm in diameter and were positioned 1600 mm away from the end of the wall, as shown in Fig. 2. Details of the column section are provided in Fig. 3(b). Longitudinal reinforcement comprised of 16×32 mm diameter bars confined by 10 mm diameter spirals spaced at 85 mm centres.

Overall thickness of the precast floor system varied between 150 mm and 175 mm with a topping thickness between 100 mm and 125 mm. Toppings were reinforced with a mesh of 12 mm diameter bars spaced



at 300 mm centres in both directions. The wall-to-floor connection was constructed as a cold joint (concrete poured against an already cured roughened concrete surface) and reinforced with 16 mm diameter bars at 450 mm centres along the length of the wall. In addition to the reinforcement in the wall-to-floor connection, drag beams provide an additional load path for the floor diaphragm loads to be transferred into the wall, as shown in Fig. 2. The drag beams were constructed within the floor system and between the PC floor units. The cross section of the drag beams was 300 mm wide and 150 mm depth reinforced with 4×20 mm diameter longitudinal bars and 6 mm diameter stirrups spaced at 100 mm centres.

The specified concrete strength, f_c' , was 40 MPa and the reinforcing steel was grade 500E, which has a nominal minimum yielding strength of 500 MPa, an ultimate to yielding stress ratio between 1.15 and 1.4 and a minimum strain at fracture of 10% [17].

3. Numerical model

A numerical model was constructed in OpenSees [18] to capture the non-linear response of the lateral load resisting system in the N-S direction of the building. The structural system was modelled using a 2D approach and subjected to a lateral pushover analysis. The model represented only a portion of the building structural system and composed of one wall and the two columns in close proximity to the end of the wall, as shown in Fig. 2(b). The lateral response of the numerical model accounted for the wall-to-floor interaction and potential coupling between the wall and the columns. The structural elements below the base (level at which the ground provides horizontal restraint) of the building were not included in the analysis nor was the portion of the wall on the 7th level (light steel structure). Both of these levels were not considered to have a significant influence on the building response for the purpose of this research.

The simulation of axial elongation of RC members is vital to accurately capture structural interactions between vertical elements. Previous work related to elongation of RC walls has shown that fibre-based models in OpenSees are able to accurately predict the global and local responses of flexure-dominant RC walls, including axial elongation [19]. Consequently, the wall and columns in the numerical model were represented with fibre-based sections, as shown in Fig. 4. The section dimensions and reinforcement were defined based on the building description provided in the previous section. The fibre-based sections were assigned to distributed-plasticity force-based beam-column elements. This element definition allows for accurate representation of both the axial-flexure interaction and the curvature along flexure dominant elements [20]. Shear deformations and bond-slip (at the wall base interface) were included according to recommendations by Oyen [21] using an aggregated material to the fibre section definition. It is worth noting that this modelling approach does not capture shear-flexure interaction and it assumes “plain sections remain plain” hypothesis. In order to properly account for the rotation of the wall section at each level and to capture the uplift at the edges of the wall panel, rigid beam elements extended from the wall centreline to the ends of the wall section, as shown in Fig. 4.

The floor system was modelled with an equivalent rectangular elastic section. The equivalent rectangular floor section was defined based on an 150 mm depth solid slab with an effective floor width and cracked inertia according to the literature [10, 13, 14, 22]. Additionally, provisions of the New Zealand Concrete Structures Standard NZS3101 [23] for cracked inertia of beams were taken into consideration. In general, these references agree that the effective slab widths vary in the range of 0.2 and 1.0 times the span length between the vertical elements and that the cracked inertia reduces to 30-40% at the ultimate state. Based on these references the width of the floor section was taken as an effective slab width equal to 30% of the span between the wall and the column and a cracked section was used with stiffness equal to 32% of the gross section properties. The coupled and uncoupled model were achieved by using either a fixed end beam element or a truss element as shown in Fig. 4(a) and Fig. 4(b) respectively.

The fibre discretisation of the element cross sections allowed for the inclusion of the confined and unconfined regions in the RC sections. The wall ends were discretised into 20 mm wide fibres and the web region into 30 mm wide fibres. Columns were discretised into fibres of a maximum size of 25×15 mm². The non-linear elements used three to four integration points to represent the plastic hinge regions as suggested by



Martinelli and Fillipou [24]. Gauss-Lobatto was used as the integration scheme for the elements. The nonlinear geometric behaviour was simulated by using a P-Delta geometric transformation assigned to each element.

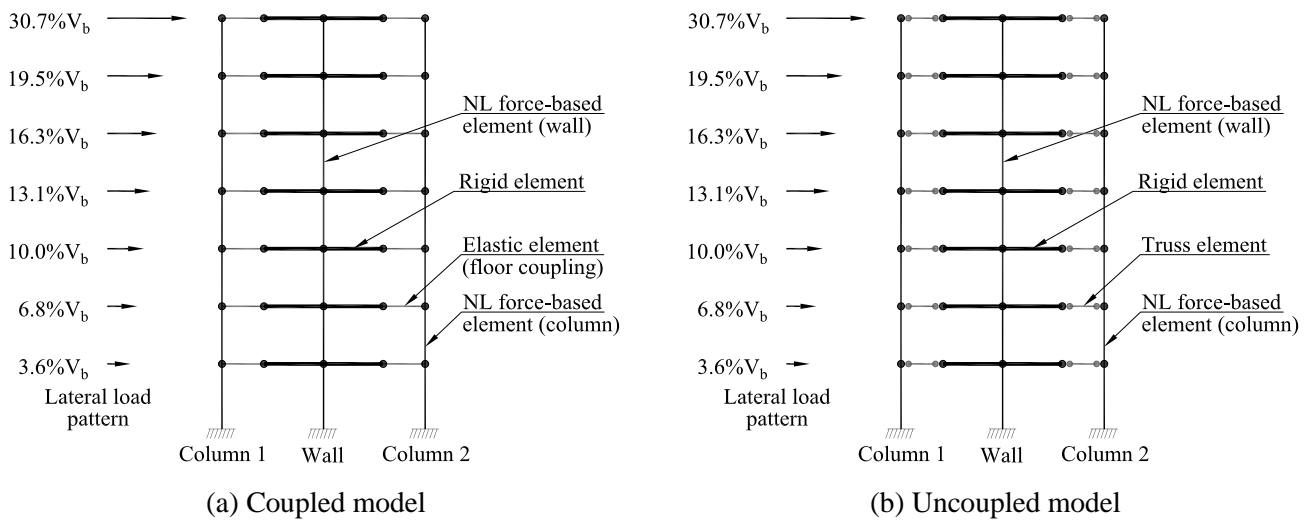


Fig. 4 – Numerical model

Uniaxial constitutive material models were used to describe the material behaviour of the fibres. Concrete in the fibre sections used the Chang and Mander [25] concrete model modified by Waugh [26] and available in OpenSees as Concrete07. The stress strain relationship of Concrete07 is shown in Fig. 5(a). It follows Tai's equation [27] until it reaches the spalling point, then it follows a straight line with the slope of the Tsai's equation at the spalling point. This concrete model provides a good representation of the inelastic concrete behaviour and considers premature crack closure creating compression stresses before the crack completely closes.

The reinforcing steel was simulated using the Menegotto and Pinto [28] model, modified by Filippou et al. [29] and available in OpenSees as Steel02. The stress-strain relationship of Steel02 is shown in Fig. 5(b). It is described by a linear elastic curve in which the slope represents the steel's elastic modulus, E_0 , then curves and follows an asymptote that represents the steel strain hardening and has a slope $b \cdot E_0$. Unloading and reloading paths are modified to capture Bauschinger effects.

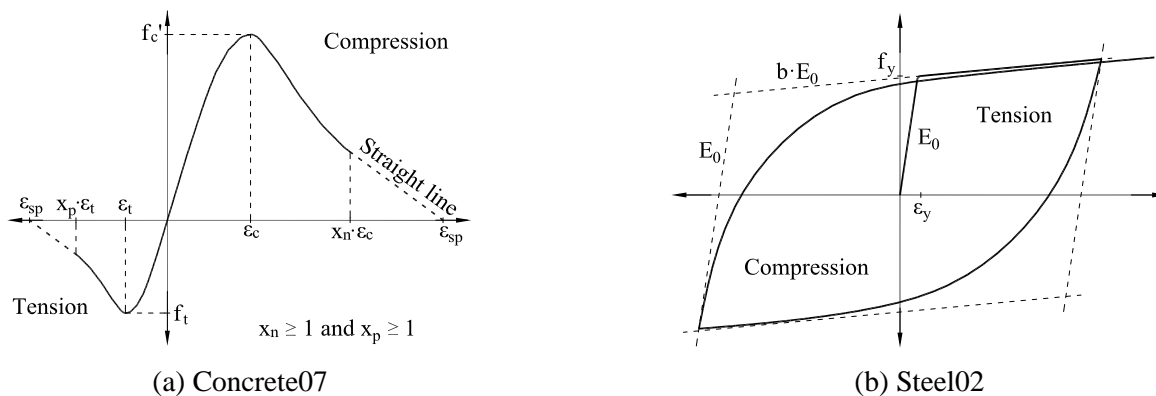


Fig. 5 – Schematic representation of constitutive material models

The unconfined concrete properties and reinforcing steel properties were based on nominal material strengths and the confined concrete properties were calculated according to the model proposed by Mander et al. [30]. Key input parameters for the material models were obtained from Collins and Mitchell [31] for unconfined



concrete in compression and from the fib 2010 Model code [32] for tensile concrete behaviour. Materials were assigned to the corresponding fibres according to their actual position in the wall and column cross-section.

Self-weight of the elements were assigned to the element nodes at each level. Imposed loads were taken from the New Zealand loading standard NZS1170.1 [33]. The imposed loads and self-weight of the floor system were transformed into equivalent nodal loads by accounting for tributary areas and were assigned at each level of the structure. The lateral load pattern to conduct the pushover analysis was taken from the Equivalent Static Method outlined in NZS1170.5 [34] and assigned at each level, as shown in Fig. 4. For calculating the lateral force distribution according to the Equivalent Static Method it was assumed that all floor levels had the same mass. The lateral target displacement was 1.5% drift at the top of the level 7.

4. Case-study building model results

The global lateral load response for the pushover analysis of the case study building model with and without structural interaction included is presented in Fig. 6. The initial stiffness of both the coupled and uncoupled systems was almost identical, with the coupled system slightly stiffer after cracking. A more significant difference was observed in the inelastic phase of the building response with a larger post-yield stiffness for the coupled building model. The strength of the lateral load resisting system was 15% stronger at 1.5% drift when compared to the strength of the uncoupled system.

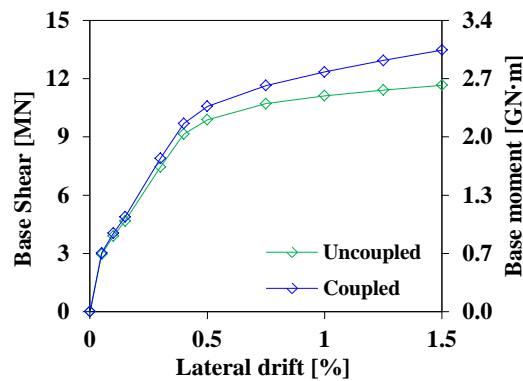


Fig. 6 – Case Study building system response with and without wall-to-floor interaction

Local response parameters were investigated to understand the increased lateral load capacity of the coupled building model, as plotted in Fig. 7 for the axial, shear and flexural demands on each component. In Fig. 7(a) it can be observed that when the model does not account for wall-to-floor interaction axial loads in both the wall and columns are constant throughout the pushover analysis. However, due to vertical displacement incompatibility between two adjacent elements and wall elongation, points that were originally at the same height move vertically relative to each other when the system is subjected to lateral displacements. When the floor coupling is modelled, this relative vertical displacement induced shear and bending actions within the floor. As a result of this coupling, part of the axial compression forces in column 1 was transferred to the wall. This process decreased the axial load on the column 1 and increased the axial load on the wall. A similar process affected the wall and column 2, where part of the axial demands on the wall was transferred to the column 2. For the coupled model, the axial demands for column 2 and the wall increased by 28% and 49% respectively when the building was subjected to 1.5% lateral drift, whereas the axial load in column 1 decreased by 67%.

Fig. 7(b) presents the moment action developed at the base of the wall. The figure illustrates that at 1.5% drift the demands on the wall increased by 4%, being similar to the uncoupled model. Since the system increased its lateral capacity by 15% at the same lateral displacement, as shown in Fig. 6, it can be derived that the additional lateral load capacity of the building was primarily provided by the column framing action (outriggers). From Fig. 7(c), the shear demand rose 13% at 1.5% drift compared to the uncoupled model. This increase in shear loads on the wall indicates that most of the additional shear actions must be resisted by the wall with little contribution of the columns.

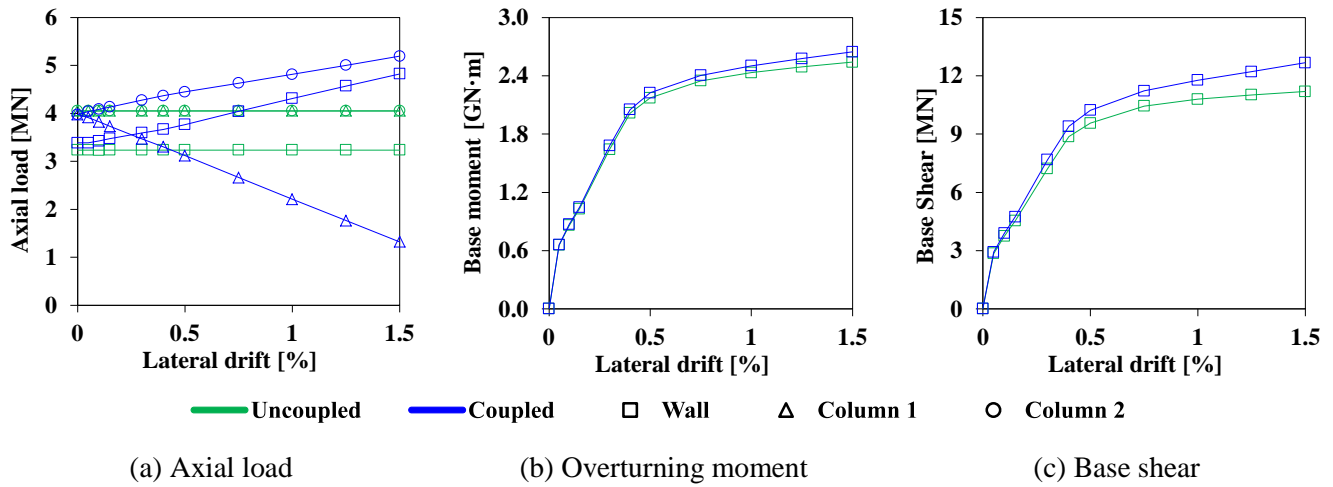


Fig. 7 – Case study building component response with and without wall-to-floor interaction

Local wall responses for both the coupled and uncoupled models are shown in Fig. 8. The moment-rotation relationship presented in Fig. 8(a) shows a progressive increase of the wall rotation in the inelastic phase. At the end of the analysis an increase of 9% in the wall base rotation can be observed in the chart. This indicates that wall-to-floor interaction caused the plastic rotation of the wall to accumulate over a shorter portion of the wall base. Despite the increase in rotation of the wall base would suggest an increase in wall elongation, the chart in Fig. 8(b) actually shows a slightly reduction in elongation between the uncoupled and coupled model. This is a result of the increased axial load acting on the wall as a consequence of wall-to-floor interaction. The larger axial load deepened the neutral axis, which not only overcame the effects of the 9% increase in rotation but reduced the elongation by 3%.

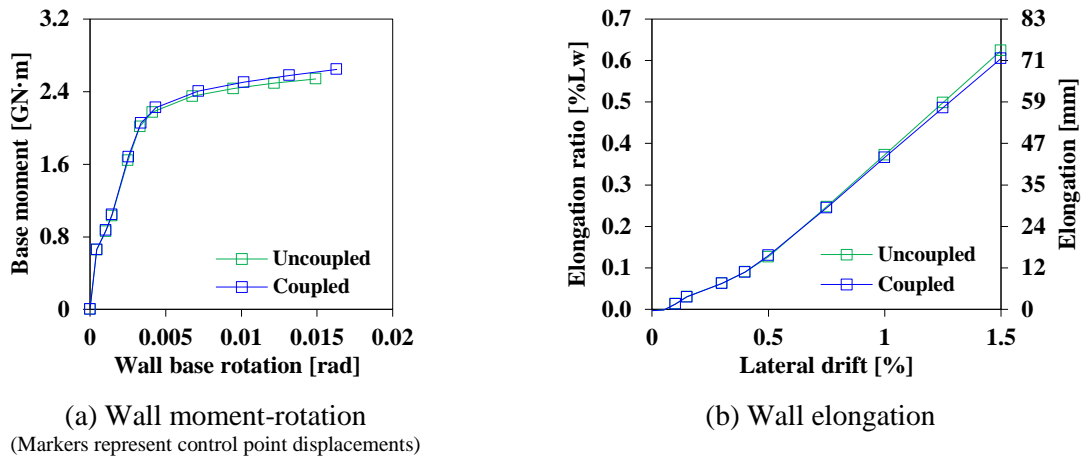


Fig. 8 – Case study building local response with and without wall-to-floor interaction



5. Parametric analyses

The parametric analysis comprised of 12 models. The models were defined based on 3 span lengths, L , between the wall and the columns and 4 effective slab widths. The cracked inertia of the sections was 32% of the gross inertia as for the previous analysis. The span lengths selected were $L = 1.6$ m, 3.2 m and 4.8 m representing one, two and three times the original model span length. Effective slab width were $0.3L$, $0.5L$, $0.7L$, $1.0L$ to represent the range proposed in the literature [10, 13, 14, 22].

Fig. 9 presents the pushover response for the parametric analyses of the lateral load resisting system. The inelastic lateral load capacity was highly influenced by the selected parameters, with a variance in results of 45% at 1.5% drift. The stiffness of the coupling elements had a significant effect on the lateral load capacity, with shorter span lengths and wider span widths increasing the coupling and lateral load capacity more significantly.

Axial, shear, and flexural demands as well as elongation and rotation for the wall are presented in Fig. 10 for each of the parametric analyses. Axial and base shear demands presented in Fig. 10(a) and Fig. 10(b) showed high variance in the results, especially for the shorter spans. For instance, at 1.5% drift the difference in axial demand between the shortest span length and largest effective width model and the longest span length and smallest effective width model was 250%. In contrast, the scatter in wall base moment, rotation and elongation was considerably smaller, as can be seen in Fig. 10(c), (d) and (e). The difference between the maximum and minimum values predicted at 1.5% drift for the wall base moment, rotation and elongation were 12%, 27% and 9%, respectively. It is observed that wall demand predictions for the models with longer spans and smaller effective slab widths were close to the predictions of the uncoupled model (black lines in the charts), mainly influenced by the reduction on stiffness produced by longer span lengths.

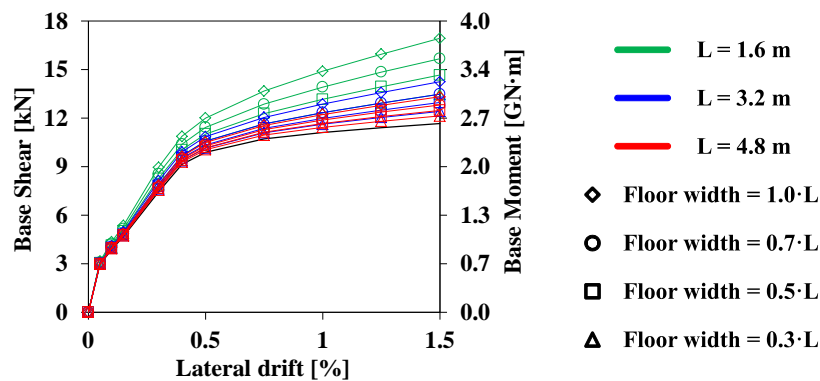


Fig. 9 – Lateral load response for parametric models

Fig. 11 presents the axial demand in the columns for each of the parametric models. Similar to the wall demands, the parametric model responses showed a large variation during the pushover analyses, especially for column 1. It can also be observed that the unloading process of the column 1 was faster for each of the parametric models than the loading process of the column 2, due to the redistribution of the axial load on column 1 towards the wall and column 2. Interesting cases for column 1 in Fig. 11(a) were those where the span length was 1.6 m and the effective slab width was larger than $0.3L$. In these cases the column completely unloaded in compression and then loaded into tension, going from 4000 kN in compression to 4200 kN in tension. Upon calculation of the maximum available shear capacity [23] provided by the coupling elements it became clear that this behaviour was not feasible because the coupling elements should have failed at lower load levels.

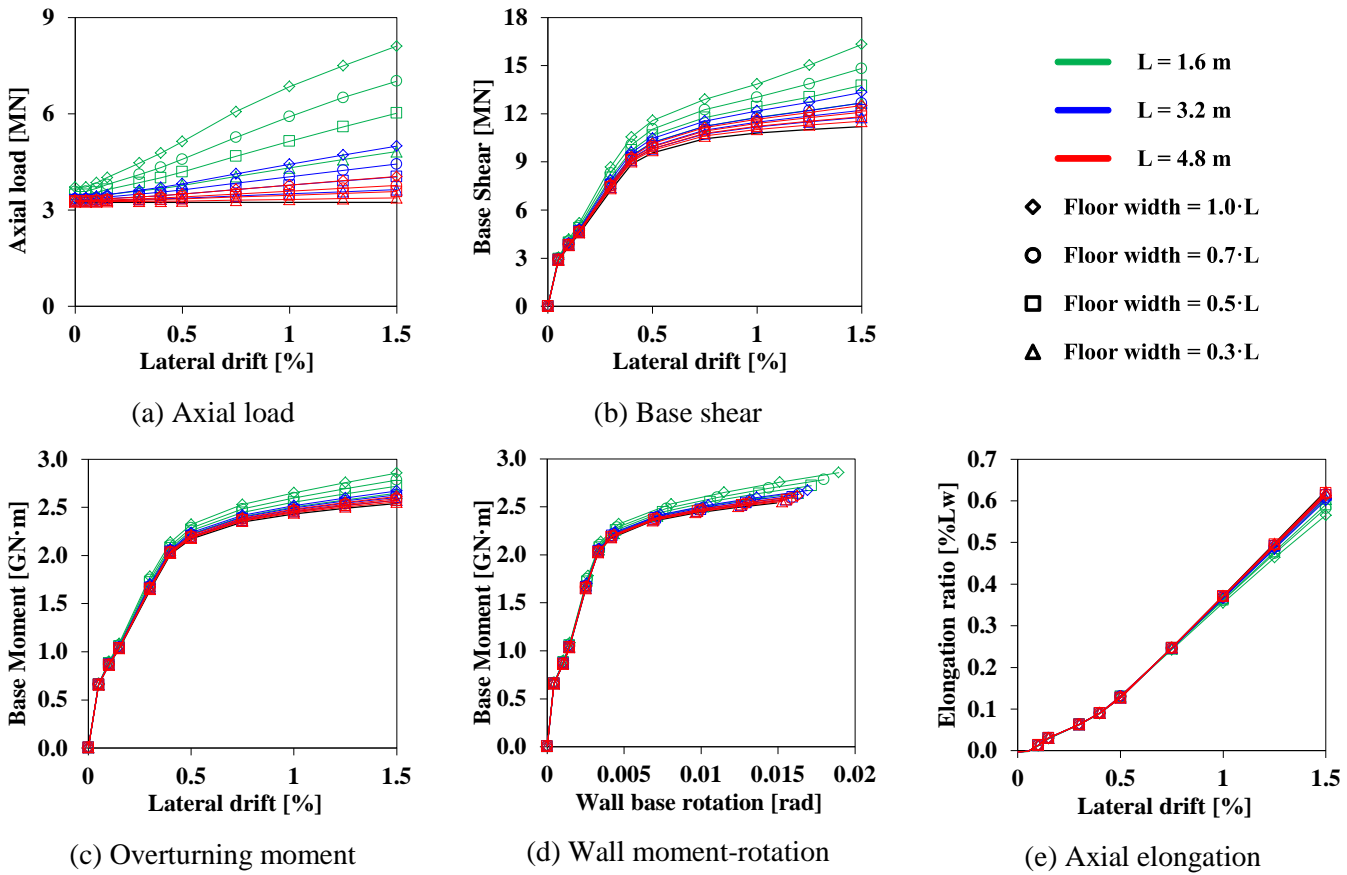


Fig. 10 – Wall response for parametric models

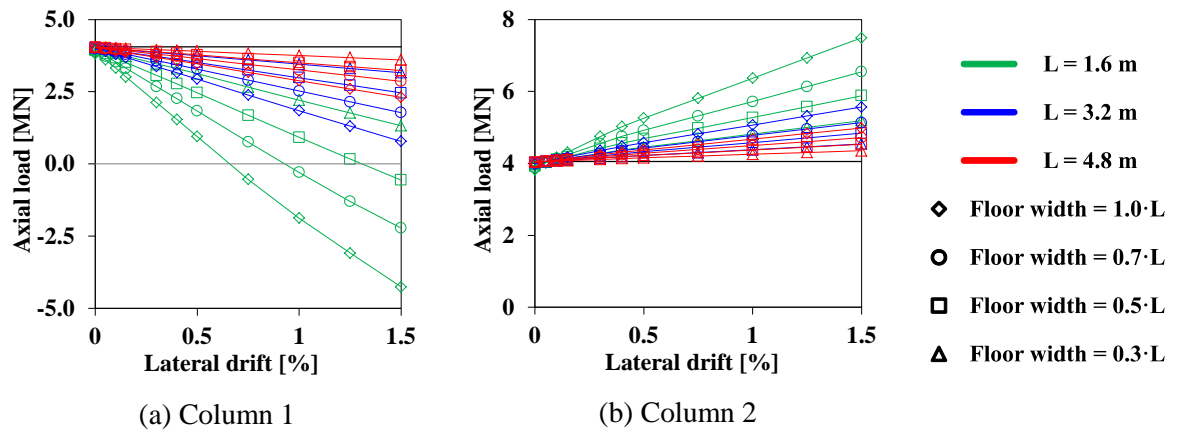


Fig. 11 – Axial demand in columns for parametric models

6. Conclusion

Floor systems may couple the response of walls with the adjacent vertical gravitational elements (wall-to-floor interaction). In order to investigate the effects of this type of structural interaction on the demands in structural components, nonlinear (NL) pushover analyses were conducted to a lateral load resisting system from an 8-storey case-study building. The lateral load resisting system was composed by a rectangular RC wall coupled with two circular columns. The floor system was modelled using an elastic equivalent rectangular element with



cracked inertia. According to the analyses performed the following preliminary conclusions about wall-to-floor interaction can be drawn:

- Wall-to-floor interaction produced axial load redistribution between the coupled elements. Comparison between the models with and without wall-to-floor interaction showed an increase in axial demands of 28% for the column 2 on the compression side, 49% increase for the wall, and a decrease in axial demand for the column 1 on the tension side of 67%.
- The lateral load resistance of the system increased by 15% when coupling was included, while the flexural demand in the wall increased by only 4%. As noticed during previous investigations [3, 16] the columns worked as outriggers adding an overturning capacity to the system.
- The base shear demands on the wall increased by 13%. Consequently, the wall was required to withstand most of the additional shear strength drawn by the increase in lateral load capacity.
- The parametric analysis showed that the response of the lateral load resisting system was highly dependent on the stiffness of the coupling elements. Differences in the order of 45% for the system lateral load capacity, and between -200% to +84% for axial load in the columns were observed amongst the parametric models analysed.
- Despite the floor system being modelled using an effective slab width with cracked inertia, unrealistic axial loads were transferred between adjacent vertical elements. Improved methodologies are needed to quantify the NL coupling behaviour of floor systems.

7. Acknowledgements

The authors wish to acknowledge the Chilean Government for awarding the first author with a BecasChile scholarship for his doctoral study at the University of Auckland and the New Zealand Concrete Society for awarding a travel bursary to support the submission and presentation of this paper. Financial support for this research was provided by the Natural Hazards Research Platform.

8. References

- [1] Priestley MJN, Paulay T (1992): *Seismic Design of Reinforced Concrete and Masonry Buildings*. John Wiley & Sons.
- [2] Wight JK (1985): *SP-84 Earthquake Effects on Reinforced Concrete Structures: U.S.-Japan Research*. American Concrete Institute.
- [3] Henry RS, Ingham J, Sritharan S (2012): Wall-to-floor interaction in concrete buildings with rocking wall systems. *NZSEE Annual Conference*, Christchurch, New Zealand.
- [4] Panagiotou M, Restrepo JJ, Conte P (2011): Shake-Table Test of a Full-Scale 7-Story Building Slice. Phase I: Rectangular Wall. *Journal of Structural Engineering*, **137**, 691-704.
- [5] Kunnath SK, Panahshahi N, Reinhorn AM (1991): Seismic Response of RC Buildings with Inelastic Floor Diaphragms. *Journal of Structural Engineering*, **117** (4), 1218-1237.
- [6] Fleischman RB, Sause R, Pessiki S, Rhodes AB (1998): Seismic Behavior of Precast Parking Structure Diaphragms. *PCI Journal*, **43** (1), 38-53.
- [7] Lee HJ, Kuchma DA (2007): Seismic Overstrength of Shear Walls in Parking Structures with Flexible Diaphragms. *Journal of Earthquake Engineering*, **11** (1), 86-109.
- [8] Bull D (2003): Understanding the Complexities of Designing Diaphragms in Buildings for Earthquakes. *Bulletin of the New Zealand Society for Earthquake Engineering*, **37** (2), 70-88.
- [9] Schwaighofer J, Collins MP (1977): Experimental Study of the Behavior of Reinforced Concrete Coupling Slabs. *ACI Journal Proceedings*, **74** (3), 123-127.
- [10] Taylor RG (1977): *The Nonlinear Seismic Response of Tall Shear Wall Structures*, Doctor of Philosophy Thesis, Department of Civil Engineering, University of Canterbury.
- [11] Coull A, Chee WY (1983): Design of floor slabs coupling shear walls. *Journal of Structural Engineering*, **109** (1), 109-125.
- [12] Paulay T, Taylor RG (1981): Slab coupling of earthquake-resisting shearwalls. *ACI Structural Journal*, **78** (2), 130-140.



- [13] Mirza MS, Lim AKW (1990): Behaviour and Design of Coupled Slab-Structural Wall Systems. *Canadian Journal of Civil Engineering*, **17** (5), 705-723.
- [14] Coull A, Chee WY (1990): Cracked Coupling Slabs in Shear Wall Buildings. *Journal of Structural Engineering*, **116** (6), 1744-1748.
- [15] Chesi C, Schnobrich WC (1987): 3-Dimensional Contribution to frame-wall Lateral Behavior. *Structural Research Series No. 531*, University of Illinois, Urbana-Champaign, U.S.A.
- [16] Waugh JD, Sritharan S (2010): Lessons Learned from Seismic Analysis of a Seven-Storey Concrete Test Building. *Journal of Earthquake Engineering*, **14** (3), 448-469.
- [17] New Zealand Standard (2001), *NZS 4671:2001 Steel Reinforcing Materials*.
- [18] Mazzoni S, McKenna F, Scott MH, Fenves GL (2006), *Open System for Earthquake Engineering Simulation (OpenSees)*, Pacific Earthquake Engineering Research Center, University of California, Berkeley, U.S.A.
- [19] Encina ER, Henry RS (2015): Preliminary Investigation of Elongation in RC walls. *NZSEE Annual Conference*, Rotorua, New Zealand.
- [20] Neuenhofer A, Filippou FC (1997): Evaluation of nonlinear frame finite-element models. *Journal of Structural Engineering*, **123** (7), 958-966.
- [21] Oyen PE (2006): *Evaluation of Analytical Tools for Determining the Seismic Response of Reinforced Concrete Shear Walls*, Master Thesis, University of Washington.
- [22] Hossain KMA (2003): Non-linear Performance of Slabs in Coupled Shear Wall Structures. *Advances in Structural Engineering*, **6** (4), 339-352.
- [23] New Zealand Standard (2006), *NZS 3101:2006 Concrete Structures Standard*.
- [24] Martinelli P, Filippou FC (2009): Simulation of the Shaking Table Test of a Seven-story Shear Wall Building. *Earthquake Engineering and Structural Dynamics*, **38**, 587-607.
- [25] Chang GA, Mander JB (1994): Seismic Energy-Based Fatigue Damage Analysis of Bridge Columns: Part 1 – Evaluation of Seismic Capacity. *NCEER-94-0006*, State University, New York, U.S.A.
- [26] Waugh J (2009): *Nonlinear analysis of T-shaped concrete walls subjected to multi-directional displacements*, Doctor of Philosophy Thesis, Department of Civil, Construction, and Environmental Engineering, Iowa State University.
- [27] Hsu TTC, Mo YL (2010): *Unified Theory of Concrete Structures*. John Wiley & Sons.
- [28] Menegotto M, Pinto PE (1973): Method of Analysis for Cyclically Loaded Reinforced Concrete Plane Frames Including Changes in Geometry and Non-Elastic Behaviour of Elements under Combined Normal Force and Bending. *Symposium of Resistance and Ultimate Deformability of Structure Acted on by Well-defined Repeated Loads*, Lisbon, Portugal.
- [29] Filippou FC, Popov EP, Bertero VV (1983): Effects of Bond Deterioration on Hysteretic Behavior of Reinforced Concrete Joints. *Technical Report UCB/EERC-83/19*, University of California, Berkeley, U.S.A.
- [30] Mander JB, Priestley MJN, Park R (1988): Theoretical Stress-Strain Model for Confined Concrete. *Journal of Structural Engineering*, **114** (8), 1804-1826.
- [31] Collins MP, Mitchell D (1997): *Prestressed Concrete Structures*.
- [32] fib (2010), *Model Code 2010 - Final Draft - Volume 1*.
- [33] New Zealand Standard (2002), *NZS 1170.1:2002 Structural Design Actions Part 1: Permanent, Imposed and other Actions*.
- [34] New Zealand Standard (2004), *NZS 1170.5:2004 Structural Design Actions Part 5: Earthquake Actions*.